

## ARTICLE

# Methanol Perturbing Modeling Cell Membranes Investigated using Linear and Nonlinear Vibrational Spectroscopy

Kangzhen Tian<sup>a</sup>, Hongchun Li<sup>b</sup>, Shuji Ye<sup>b,c\*</sup>*a. Department of Physics, University of Science and Technology of China, Hefei 230026, China**b. Department of Chemical Physics, University of Science and Technology of China, Hefei 230026, China**c. Hefei National Laboratory for Physical Sciences at the Microscale, University of Science and Technology of China, Hefei 230026, China*

(Dated: Received on November December 7, 2012; Accepted on January 5, 2013)

Cell membranes play a crucial role in many biological functions of cells. A small change in the composition of cell membranes can strongly influence the functions of membrane-associated proteins, such as ion and water channels, and thus mediate the chemical and physical balance in cells. Such composition change could originate from the introduction of short-chain alcohols, or other anesthetics into membranes. In this work, we have applied sum frequency generation vibrational spectroscopy (SFG-VS), supplemented by attenuated total reflectance Fourier transform infrared spectroscopy (ATR-FTIR), to investigate interaction between methanol and 1,2-dimyristoyl-d54-sn-glycero-3-phosphocholine (d54-DMPC) lipid bilayers. Lipid's hydrocarbon interior is deuterated while its head group is hydrogenated. At the same time, CH<sub>3</sub> symmetric stretch from methanol and lipid head amine group has different frequency, thus we can distinguish the behaviors of methanol, lipid head amine group, and lipid hydrocarbon interior. Based on the spectral feature of the bending mode of the water molecules replaced by methanol, we determined that the methanol molecules are intercalated into the region between amine and phosphate groups at the lipid hydrophilic head. The dipole of CH<sub>3</sub> groups of methanol and lipid head, and the water O-H all adopt the same orientation directions. The introduction of methanol into the lipid hydrophilic head group can strongly perturb the entire length of the alkyl chains, resulting that the signals of CD<sub>2</sub> and CD<sub>3</sub> groups from both leaflets can not cancel each other.

**Key words:** Sum frequency generation vibrational spectroscopy, Cell membrane, Methanol, Interaction, Mechanism

## I. INTRODUCTION

Cell membranes play a crucial role in many biological functions of cells. They govern all interactions between cells and their environments, such as the exchange of information and ions/molecules between the inside and outside of the cells. A variety of peptides and proteins are embedded inside or associated with the cell membranes, helping to fulfill various cellular functions [1–3]. A small change in the composition of cell membranes can strongly influence the functions of these embedded membrane proteins, such as ion and water channels, and thus mediate the chemical and physical balance in cells [4–6]. Such composition change could originate from the introduction of short-chain alcohols, or other anesthetics into membranes [6]. It has been recognized that high alcohol concentrations modify the membrane

structure and cause the unfavorable conformation transition of transmembrane proteins [6–8]. Alcohol has been also suggested to promote an early stage of membrane hemifusion [9, 10].

In addition to the wide use in anesthetic agents and disinfectants, short-chain alcohols are often used as solvents to dissolve the water-insoluble proteins/peptides, such as alamethicin and islet amyloid polypeptide, to study the structures and kinetics of membrane-associated proteins. Therefore, the effects of alcohols on membranes are very important in many biological and medical applications. Although the alcohol-membrane interaction has been previously studied by various experimental and theoretical approaches [6–9, 11–27], those studies so far mainly focused on the influences of alcohols on properties of membranes such as alcohol partition coefficients into membranes [6–9, 11–30]. Yet the mechanisms by which the interaction between alcohols and cell membranes at the molecular level are still not completely understood.

Since planar substrate-supported lipid bilayer has

\* Author to whom correspondence should be addressed. E-mail: shujiye@ustc.edu.cn, Tel./FAX: +86-551-63603462

been widely used as a model to mimic cell membranes, in this research, we applied sum frequency generation vibrational spectroscopy (SFG-VS), supplemented by attenuated total reflectance Fourier transform infrared spectroscopy (ATR-FTIR), to investigate interaction between methanol and 1,2-dimyristoyl-d54-sn-glycero-3-phosphocholine (d54-DMPC) lipid bilayer. SFG-VS is a powerful and highly versatile spectroscopic tool for identifying interfacial molecular species (or chemical groups) and measuring the orientation of functional groups on a surface or at an interface in different chemical environments [31–49]. We used d54-DMPC to prepare lipid bilayer because its hydrocarbon interior is deuterated while head group is hydrogenated. At the same time, the  $\text{CH}_3$  symmetric stretch modes from methanol and lipid head amine groups have different frequency. Thus we can distinguish the behaviors of methanol, lipid head amine group, and lipid hydrocarbon interior. Here, we focused on the molecular structure change of lipid bilayer perturbed by the introduction of methanol molecules.

## II. EXPERIMENTS

### A. Materials and sample preparations

d54-DMPC lipids were purchased from Avanti Polar Lipids (Alabaster, AL). Methanol, betaine, and poly(ethylene glycol) with average molecular weight of 200 (PEG 200) were purchased from Sigma-Aldrich with a minimum purity of 98%. Chemical structures of d54-DMPC, betaine, and PEG 200 are shown in Fig.1. Right-angle  $\text{CaF}_2$  prisms were purchased from Chengdu Ya Si Optoelectronics Co., Ltd (Chengdu, China). All of the chemicals were used as received. The phospholipid was dissolved in chloroform and kept at  $-20\text{ }^\circ\text{C}$ .

$\text{CaF}_2$  prisms were thoroughly cleaned using a procedure with several steps. They were first soaked in toluene for at least 24 h and then sonicated in soap detergent solution for 0.5 h. After that, they were rinsed with deionized (DI) water before soaking in methanol for 10 min. All of the prisms were then rinsed thoroughly with an ample amount of DI water and cleaned inside Harrick plasma chamber for 10 min immediately before depositing lipid molecules on them. Substrates were tested using SFG and no signal from contamination was detected.

Single lipid bilayer was prepared on  $\text{CaF}_2$  substrates using Langmuir-Blodgett and Langmuir-Schaefer (LB/LS) methods with a KSV mini trough LB system. Ultrapure water from a Milli-Q reference system (Millipore, Bedford, MA) was used throughout the experiments for bilayer preparation. The detailed procedure was similar to previous reports [50–52]. The bilayer was immersed in water inside a 2-mL reservoir throughout the entire experiment. For methanol-bilayer interaction experiments,  $\sim 50\text{ }\mu\text{L}$  methanol

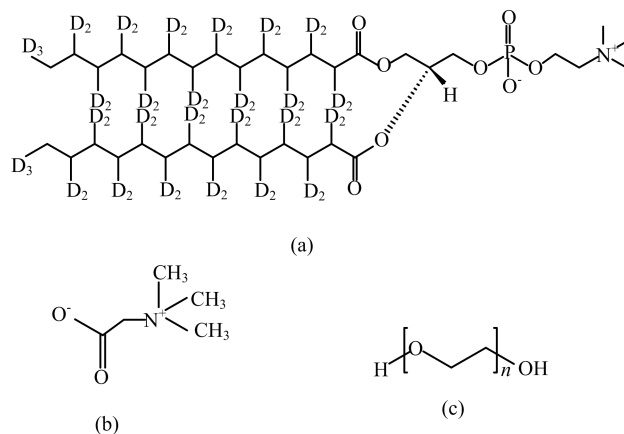


FIG. 1 Chemical structure of (a) d54-DMPC, (b) betaine, and (c) PEG 200.

(with a mole fraction of 0.011) was injected into the reservoir. A magnetic microstirrer was used to ensure a homogeneous concentration distribution of methanol molecules in the subphase below the bilayer.

### B. Polarized ATR-FTIR experiments

A Shimadzu IRPrestige-21 spectrometer was used to collect ATR-FTIR spectra with a standard  $45^\circ$  ZnSe ATR cell (Specac Ltd. Woodstock, GA) and a ZnSe grating polarizer (PIKE Technologies, Inc., Masison, WI). The ZnSe crystal (Specac Ltd. Woodstock, GA) was cleaned using the same procedures as the  $\text{CaF}_2$  prisms. The lipid bilayer was prepared onto the ZnSe crystal surface using the LB/LS method mentioned above. After the lipid bilayer was deposited onto the crystal and kept stable at least 2 h to allow equilibration, a background polarized spectrum of the lipid bilayer/ $\text{H}_2\text{O}$  interface was recorded. Then about  $40\text{ }\mu\text{L}$  methanol (with a mole fraction of 0.011) were injected into the small reservoir of 1.6 mL. After at least 1 h to allow the methanol adsorption to reach equilibrium, a polarized spectrum was collected. Finally, the signal of methanol on bilayer in  $\text{H}_2\text{O}$  was obtained by subtracting the background spectrum of the bilayer/ $\text{H}_2\text{O}$  interface from the later collected spectrum after methanol was adsorbed and equilibrated. All the spectra collected here were averages of 256 scans with a  $2\text{ cm}^{-1}$  resolution.

### C. SFG-VS experiments

Details regarding SFG-VS theories and instruments have been reported previously [32–49]. The SFG setup is similar to that described in our earlier publications [53, 54]. In this research, all SFG-VS experiments were carried out at the room temperature ( $24\text{ }^\circ\text{C}$ ). SFG spectra from interfacial lipid bilayer and methanol

with different polarization combinations including ssp (s-polarized SFG output, s-polarized visible input, and p-polarized infrared input) were collected using the near total internal reflection geometry. All SFG spectra were averaged over 100 times at each point and normalized by the intensities of the input IR and visible beams.

#### D. Fitting of SFG-VS signals

As described in detail elsewhere [32–49], the intensity of the SFG light is related to the square of the sample's second-order nonlinear susceptibility ( $\chi_{\text{eff}}^{(2)}$ ), and the intensity of the two input fields  $I(\omega_{\text{IR}})$  and  $I(\omega_{\text{vis}})$ , see Eq.(1), which vanishes when a material has inversion symmetry.

$$I(\omega_{\text{SFG}}) \propto t|\chi_{\text{eff}}^{(2)}|^2 I_1(\omega_{\text{vis}}) I_2(\omega_{\text{IR}}) \quad (1)$$

$$\omega_{\text{SFG}} = \omega_{\text{IR}} + \omega_{\text{vis}} \quad (2)$$

As the IR beam frequency is tuned over the vibrational resonance of surface/interface molecules, the effective surface resonant nonlinear susceptibility  $\chi_{\text{R}}^{(2)}$  can be enhanced. The frequency dependence of  $\chi_{\text{eff}}^{(2)}$  is described by Eq.(3)

$$\begin{aligned} \chi_{\text{eff}}^{(2)}(\omega) &= \chi_{\text{NR}}^{(2)} + \chi_{\text{R}}^{(2)} \\ &= \chi_{\text{NR}}^{(2)} + \sum_v \frac{A_v}{\omega - \omega_v + i\Gamma_v} \end{aligned} \quad (3)$$

where  $A_v$ ,  $\omega_v$ , and  $\Gamma_v$  are the strength, resonant frequency, and damping coefficient of the vibrational mode ( $v$ ), respectively.  $A_v$  could be either positive or negative depending on the phase of the vibrational mode with respect to the nonresonant background  $\chi_{\text{NR}}^{(2)}$ . The plot of SFG signal *vs.* the IR input frequency shows a polarized vibrational spectrum of the molecules at surface or interface.  $A_v$ ,  $\omega_v$ , and  $\Gamma_v$  can be extracted by fitting the spectrum.

### III. RESULTS AND DISCUSSION

#### A. ATR-FTIR results

FTIR is a sensitive technique which can permit to identify the vibrational state of molecular species (or chemical groups). It has been widely applied to study the structural and dynamic properties of biological membranes in different chemical environments [55, 56]. FTIR has also been used to study the interaction between alcohols and the reversed micelle or liposome system [11, 12, 55, 57]. Earlier studies suggested that short-chain alcohol (methanol, ethanol, or *n*-butanol) mainly binds with phospholipid bilayer at the lipid-water interface rather than in the hydrocarbon interior [14, 17, 30]. Molecular dynamics simulations indicated short-chain alcohols are able to penetrate through

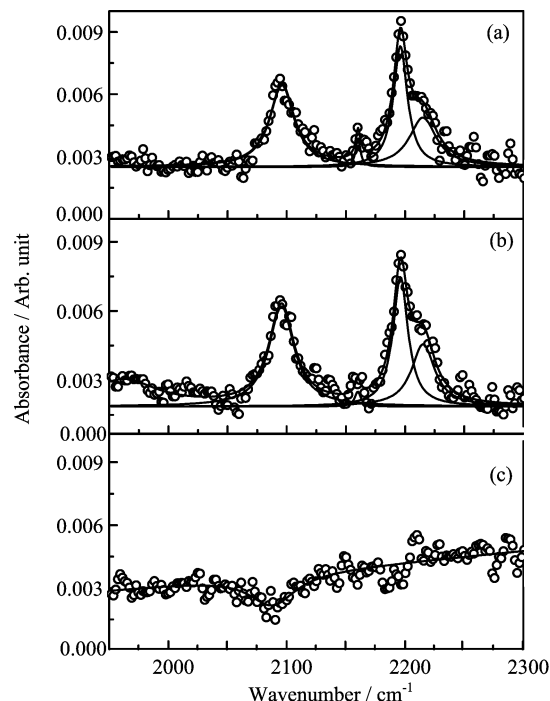


FIG. 2 (a) The s polarized and (b) p polarized ATR-FTIR spectra of d54-DMPC/d54-DMPC bilayer, (c) s polarized ATR-FTIR spectra difference after adding methanol. Open circles show the experimental data, solid lines represent the fitting profile.

the membrane [6]. Here we studied the interaction between planar substrate-supported d54-DMPC/d54-DMPC lipid bilayer by using polarized ATR-FTIR spectra. The spectra of d54-DMPC/d54-DMPC lipid bilayer and the spectra difference after adding methanol were presented in Fig.2. Before injecting methanol, ATR-FTIR spectra of d54-DMPC/d54-DMPC lipid bilayer are dominated by the peaks at 2096, 2160, 2196, and 2215  $\text{cm}^{-1}$ , which are contributed by the  $\text{CD}_2$  symmetric stretch,  $\text{CD}_2$  Fermi resonance,  $\text{CD}_2$  asymmetric stretch, and  $\text{CD}_3$  asymmetric stretch, respectively [56]. The intensity ratio of the signal measured using the p-versus s- polarized beam for the 2096  $\text{cm}^{-1}$  peak is 1.1. Assuming a  $\delta$  orientation distribution, the orientation angle is determined to be  $\theta=40^\circ$  for  $\text{CD}_2$  molecular direction. After injecting methanol (with a mole fraction of 0.011) and reaching equilibration, we measured the spectra difference before and after injecting methanol. Figure 2(c) indicated that methanol can only induce a tiny spectra loss centered at about 2096  $\text{cm}^{-1}$ .

Figure 3 shows the spectra difference after injecting methanol and reaching equilibration, seven positive peaks at 1016, 1112, 1405, 1450, 2843, 2920, and 2955  $\text{cm}^{-1}$  and one broad negative peak at 1625  $\text{cm}^{-1}$  were detected. The positive peaks are originated from the C–O symmetric stretch,  $\text{CH}_3$  deformation, COH symmetric bending,  $\text{CH}_3$  symmetric bending,  $\text{CH}_3$  symmetric stretch,  $\text{CH}_3$  Fermi resonance, and  $\text{CH}_3$  asym-

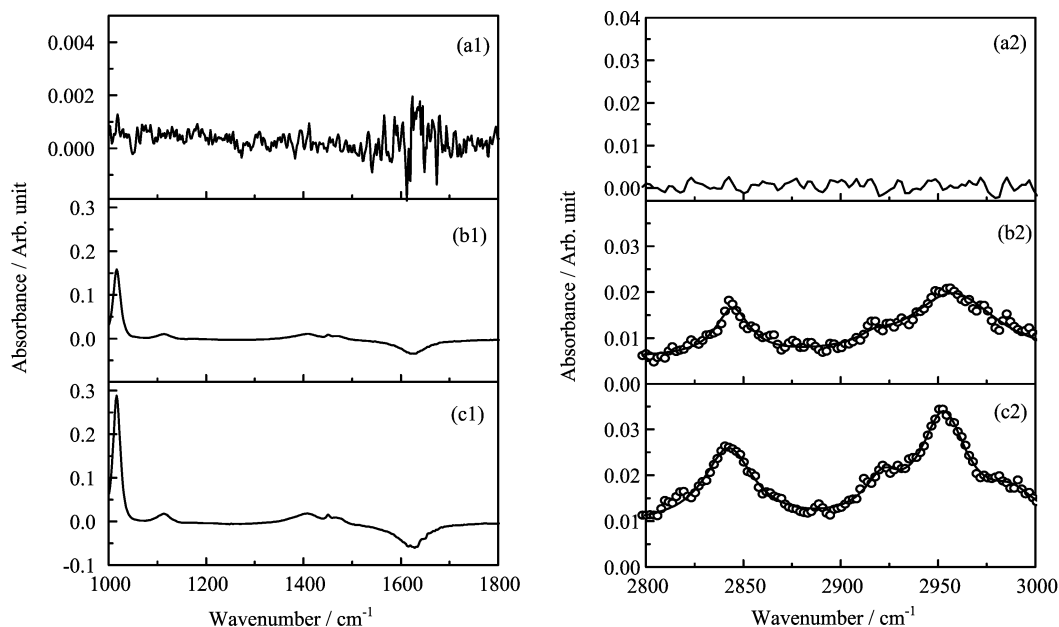


FIG. 3 ATR-FTIR spectra difference before and after adding methanol. (a) s polarized spectra difference before adding methanol, (b) s polarized spectra difference after adding methanol, (c) p polarized spectra difference after adding methanol. For (a1), (b1), (c1), and (a2) solid curves show the experimental data. For (b2) and (c2) open circles show the experimental data and solid lines represent the fitting profile.

metric stretch of methanol, respectively [58]. The peak center of these modes is consistent with the value reported in dilute methanol aqueous solution with the mole fraction of methanol  $x < 0.1$  [58, 59].

It is interesting to observe that one broad negative peak was detected at  $1625\text{ cm}^{-1}$  (Fig.4 (d) and (e)). The negative peak is assigned as water bending mode. Previous studies suggested that short-chain alcohols (up to three carbon atom) mainly interact with the membrane by competing with water for hydration sites of the lipid hydrophilic head [11, 12, 17, 54, 56]. The membrane-bound water was replaced by methanol molecules and thus a negative signal appeared. Generally, the normal  $\text{H}_2\text{O}$  bending mode occurs at  $1640\text{--}1645\text{ cm}^{-1}$ , as shown in Fig.4(a). However, the bending mode of the membrane-bound water shifts to  $1625\text{ cm}^{-1}$ . To clarify the origination of the peak shift, we measured the water bending mode in PEG 200 and betaine aqueous solution on ZnSe ATR crystal, which shows the peak center at  $1637$  and  $1627\text{ cm}^{-1}$ , respectively, as shows in Fig.4 (b) and (c). Betaine is a specific type of Zwitterion while PEG 200 has a  $-\text{CH}_2\text{CH}_2\text{O}-$  moiety. Zwitterionic and  $-\text{CH}_2\text{CH}_2\text{O}-$  moieties can both form strong hydration bond with water. They give different frequency of the water bending, indicating these two types of hydration bonds are different. The bending mode of the membrane-bound water has the similar peak center with the one of betaine aqueous solution. Therefore we believe the  $1625\text{ cm}^{-1}$  peak is possibly contributed by the bound water at the region between the cationic

(amine) and anionic (phosphate) groups of the lipid hydrophilic head, which may indicate that the methanol locates at the amine-phosphate moiety and replaces the membrane-bound water position. The peak shift is further confirmed by the bilayer/ $\text{D}_2\text{O}$  system (in Fig.4 (f) and (g)), where the lipid-bound  $\text{D}_2\text{O}$  bending mode occurs at  $1190\text{ cm}^{-1}$  while the normal  $\text{D}_2\text{O}$  bending mode has the frequency at  $1215\text{ cm}^{-1}$  [56].

## B. SFG-VS results

Figure 5 presents the ssp SFG spectra of d54-DMPC/d54-DMPC bilayer in the absence and presence of methanol. Before adding methanol, very weak signals at  $2095$ ,  $2205$ ,  $2875$ , and  $2940\text{ cm}^{-1}$  were observed. The peaks at  $2095$  and  $2205\text{ cm}^{-1}$  originate from symmetric stretch and asymmetric stretch of  $\text{CD}_2$  group respectively [33]. Weak C–D signals from isotopically symmetric bilayer indicate that the proximal leaflet and distal leaflet have very similar structures and signals generated from both leaflets effectively canceled each other. The peaks at  $2875$  and  $2940\text{ cm}^{-1}$  come from the  $\text{CH}_3$  symmetric stretch and Fermi resonance of the hydrophilic head group of d54-DMPC lipid.

After adding methanol at least 1 h and reaching equilibrium, we measured the ssp spectra again (Fig.5 (b) and (d)). Several strong peaks appear at  $2070$ ,  $2095$ ,  $2110$ ,  $2170$ ,  $2220$ ,  $2850$ ,  $2875$ ,  $2930$ ,  $2940$ , and  $2955\text{ cm}^{-1}$ . The peaks at  $2070$ ,  $2110$ , and  $2220\text{ cm}^{-1}$  are attributed to  $\text{CD}_3$  symmetric stretch,  $\text{CD}_3$  Fermi

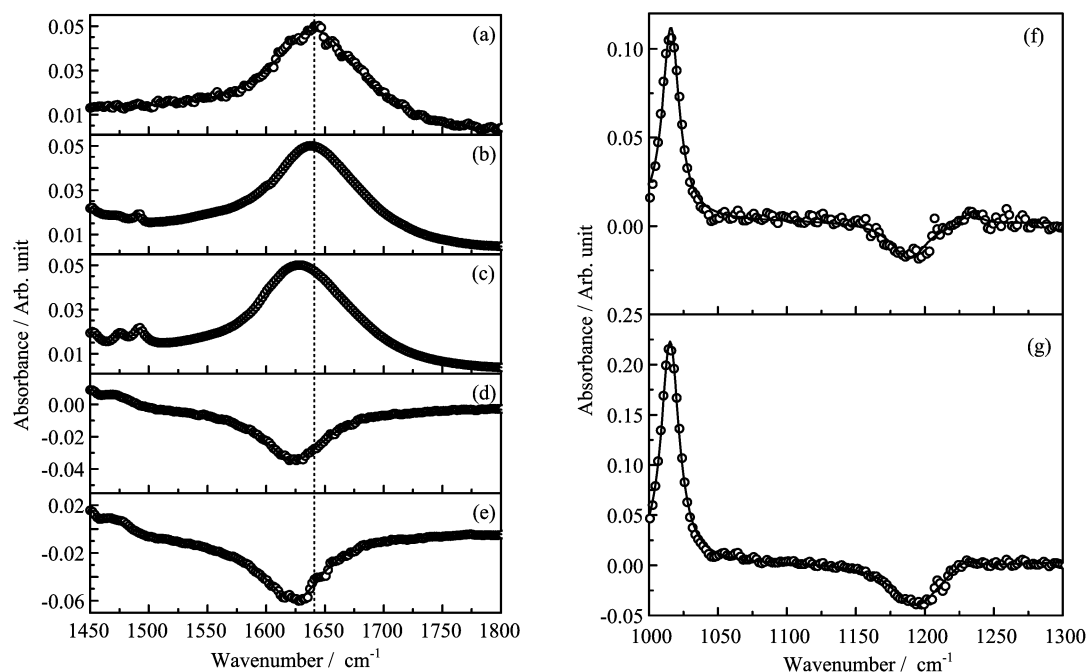


FIG. 4 ATR-FTIR spectra of water on ATR crystal, (a) pure water, (b) PEG 200 solution, (c) betaine solution, (d) lipid bilayer in  $\text{H}_2\text{O}$  after adding methanol, s polarization, (e) lipid bilayer in  $\text{H}_2\text{O}$  after adding methanol, p polarization, (f) lipid bilayer in  $\text{D}_2\text{O}$  after adding methanol, s polarization, (g) lipid bilayer in  $\text{D}_2\text{O}$  after adding methanol, p polarization. Open circles show the experimental data and solid lines represent the fitting profile.

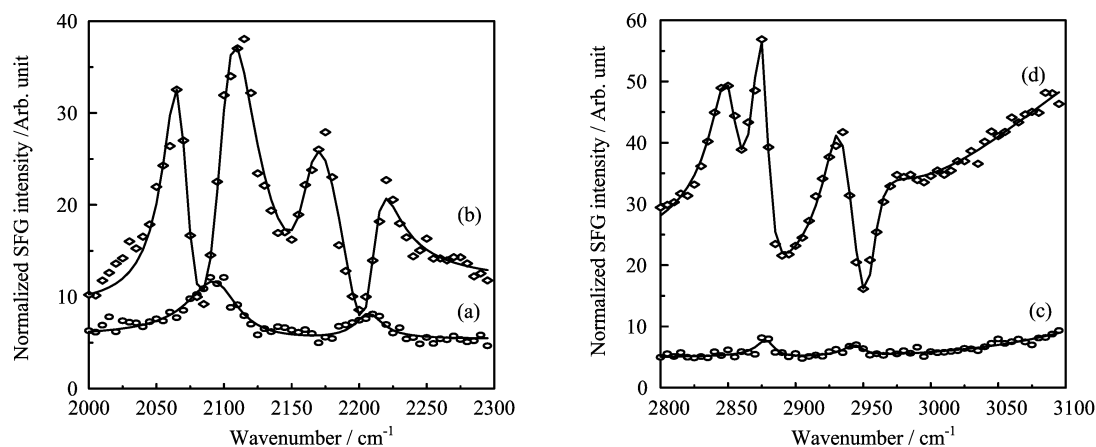


FIG. 5 SFG spectra of DMPC bilayer with ssp polarization. (a) and (c) in the absence of methanol, (b) and (d) in the presence of methanol.

resonance, and  $\text{CD}_3$  asymmetric stretch, respectively. The  $2170\text{ cm}^{-1}$  peak is assigned to  $\text{CD}_2$  Fermi resonance. The signal from  $\text{CD}_2$  is much stronger than the signal before adding methanol. The appearance of the peaks at  $2070$ ,  $2110$ , and  $2220\text{ cm}^{-1}$  indicated that the alkyl chains were strongly perturbed by methanol molecules. This effect is most likely caused by the intercalation of methanol into the region between amine and phosphate groups at the lipid hydrophilic head, increasing the spacing between lipids in outer leaflets. Thus the signals generated from both leaflets can not cancel each other. Previous NMR study on the interaction between

ethanol and lipid bilayer also suggested that the interfacial binding of ethanol is capable of disordering the entire length of the alkyl chains, which could explain the small alcohol-induced fluidization of membrane lipids that has been frequently reported in Ref.[14].

The SFG spectra of methanol have been well studied [60–64]. The SFG spectra of methanol solution with mole fraction of 0.03 are dominated by the peaks at  $2843\text{ cm}^{-1}$  ( $\text{CH}_3$  symmetric stretch, strong),  $2925\text{ cm}^{-1}$  ( $\text{CH}_3$  Fermi resonance, weak),  $2955\text{ cm}^{-1}$  ( $\text{CH}_3$  asymmetric stretch, medium). It is also found that there is a red-shift of the  $\text{CH}_3$  symmetric stretch frequency of

TABLE I Fitting parameters of the SFG spectra in Fig.5(d). The errors of the fitting parameters are given in parenthesis.

$\omega_v/\text{cm}^{-1}$	$A_v$	$\Gamma_v$
2850	33.4(1.4)	12.8(0.5)
2875	28.3(0.7)	7.3(0.2)
2930	36.6(4.0)	13.2(0.6)
2940	20.7(5.4)	12.3(0.5)
2955	-69.1(3.0)	10.5(0.3)
3170	1184(17.7)	181(2.1)

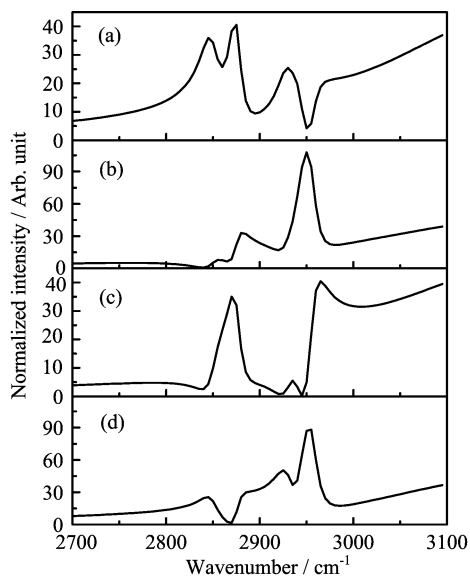


FIG. 6 The simulated SFG spectral profile with different phase signs given in Table II.

methanol with the increase of methanol concentration observed by SFG due to a changing hydrogen bonding configuration between the methanol and the water molecules at the surface and in the bulk. Based on the relationship between the peak center and methanol concentration, the peak center of  $\text{CH}_3$  symmetric stretch is deduced to be  $2847 \text{ cm}^{-1}$  at mole fraction of 0.01, which is close to present peak observed at  $2850 \text{ cm}^{-1}$ . Therefore, we believe the peaks at  $2850$  and  $2930 \text{ cm}^{-1}$  should come from  $\text{CH}_3$  symmetric stretch and Fermi resonance of methanol. The peaks at  $2875$ ,  $2940$ , and  $2955 \text{ cm}^{-1}$  are attributed to  $\text{CH}_3$  symmetric stretch, Fermi resonance, and asymmetric stretch of the hydrophilic head group of d54-DMPC lipid. Because of insertion of methanol, the symmetry of lipid hydrophilic head group was broken, resulting in a great enhancement of the signal from lipid amine  $\text{CH}_3$  group. The tail signal in Fig.5(d) comes from the interfacial water.

The molecular orientation information of the function group can be obtained by relating SFG susceptibility tensor elements  $\chi_{ijk,q}^{(2)}$  ( $i, j, k=x, y, z$ ) to the SFG molecular hyperpolarizability tensor elements  $\beta_{lmn,q}$  ( $l, m, n=a, b, c$ ) via the Euler transformation, or qual-

TABLE II Spectral parameters for the simulated SFG spectra in Fig.6.

$\omega_v/\text{cm}^{-1}$	$A_v$	$\Gamma_v$	Phase sign			
			(a)	(b)	(c)	(d)
2850	30	12	+	+	-	-
2875	30	8	+	+	+	+
2930	30	12	+	+	-	-
2940	15	8	+	+	+	+
2955	60	10	-	-	-	-
3170	1200	180	+	-	+	-

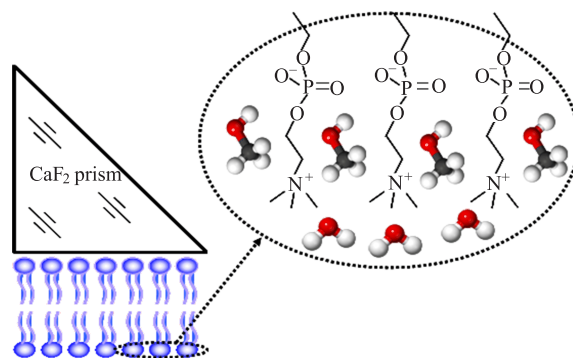


FIG. 7 A scheme of the location of methanol in lipid bilayer.

itatively determined in terms of the phase of the vibrational mode [32–49]. To qualitatively determine the phase of  $\text{CH}_3$  symmetric stretch mode of methanol molecules, we fitted the spectra in Fig.5(d) using Eq.(1). The fitting parameters are present in Table I. It is found that the phase signs which give a best fitting are all positive for  $\text{CH}_3$  symmetric stretch mode of methanol,  $\text{CH}_3$  symmetric stretch mode of lipid head group, and water O–H stretch mode, which is further confirmed by Fig.6, where we simulated the spectral profile using the assuming parameters given in Table II. Generally, the symmetric stretch and Fermi resonance modes have the same phase, while symmetric stretch and asymmetric stretch modes have opposite phase. Therefore, there are only four combinations of the phase signs. As indicated by Fig.5 and Fig.6, only if  $\text{CH}_3$  symmetric stretch of methanol,  $\text{CH}_3$  symmetric stretch of lipid head group, and water O–H stretch modes all adopt the same sign, the simulated spectra have similar profile with the experimental results. This result suggests that the dipole of  $\text{CH}_3$  group in methanol and lipid head, and the water O–H all have the same orientation directions. All orient toward the bulk water (shown in Fig.7). In fact, previous phase sensitive SFG study has proven that the water O–H stretch and amine  $\text{CH}_3$  group of neutral lipid both orient toward the same direction [65].

#### IV. CONCLUSION

We have applied SFG-VS, supplemented by ATR-FTIR, to investigate interaction between methanol and d54-DMPC lipid bilayer. Based on the spectral feature of the bending mode of the water molecules replaced by methanol, we successfully determined that the methanol molecules are intercalated into the region between amine and phosphate groups at the lipid hydrophilic head. The dipole of CH<sub>3</sub> group in methanol and lipid head, and the water O–H all adopt the same orientation directions. The introduction of methanol into the lipid hydrophilic head group can strongly perturb the entire length of the alkyl chains, resulting that the signals of CD<sub>2</sub> and CD<sub>3</sub> groups generated from both leaflets can not cancel each other. Results from our studies will aid in understanding the mechanism of introduction of short-chain alcohols, or other anesthetics into membranes at molecular-level, as well as the mechanism of the effect of alcohol on cellular systems such as bacteria and yeast.

#### V. ACKNOWLEDGMENTS

This work was supported by the National Natural Science Foundation of China (No.21273217 and No.91127042), the National Basic Research Program of China (No.2010CB923300), and the Knowledge Innovation Program of the Chinese Academy of Sciences (KJ CX2-EW-W09). Shuji Ye thanks Prof. Yi Luo at USTC for his kind help and discussion.

- [1] J. Katsaras and T. Gutberlet, *Lipid Bilayers: Structure and Interactions*, New York: Springer, (2001).
- [2] C. R. Mateo, J. Gómez, J. Villalaín and J. M. González Ros, *Protein-Lipid Interaction: New Approaches and Emerging Concepts*, Berlin: Springer, (2006).
- [3] P. L. Yeagle, *The Structure of Biological Membranes*, Boca Raton, FL: CRC Press, (2005).
- [4] R. S. Cantor, *Biochemistry* **42**, 11891 (2003).
- [5] A. R. Mazzeo, J. Nandi, and R. A. Levine, *Am. J. Physiol.* **254**, G57 (1988).
- [6] M. Patra, E. Salonen, E. Terama, I. Vattulainen, R. Faller, B. W. Lee, J. Holopainen, and M. Karttunen, *Biophys. J.* **90**, 1121 (2006).
- [7] M. Weis, M. Kopani, J. Jakubovsky, and L. Danihel, *Appl. Surf. Sci.* **253**, 2425 (2006).
- [8] D. Pinisetty, D. Moldovan, and R. Devireddy, *Annals Biomed. Eng.* **34**, 1442 (2006).
- [9] A. A. Gurtovenko and J. Anwar, *J. Phys. Chem. B* **113**, 1983 (2009).
- [10] A. Chanturiya, E. Leikina, J. Zimmerberg, and L. V. Chernomordik, *Biophys. J.* **77**, 2035 (1999).
- [11] J. S. Chiou, P. R. Krishna, H. Kamaya, and I. Ueda, *Biochim. Biophys. Acta* **1110**, 225 (1992).
- [12] J. A. Centeno and T. J. O'Leary, *Biochemistry* **29**, 7289 (1990).
- [13] P. Westh, C. Trandum, and Y. Koga, *Biophys. Chem.* **89**, 53 (2001).
- [14] J. A. Barry and K. Gawrisch, *Biochemistry* **33**, 8082 (1994).
- [15] J. A. Barry and K. Gawrisch, *Biochemistry* **34**, 8852 (1995).
- [16] B. W. Koenig and K. Gawrisch, *J. Phys. Chem. B* **109**, 7540 (2005).
- [17] U. Wanderlingh, G. D'Angelo, V. C. Nibali, C. Crupi, S. Rifici, C. Corsaro, and G. Sabatino, *Spectroscopy* **24**, 375 (2010).
- [18] M. F. N. Rosser, H. M. Lu, and P. Dea, *Biophys. Chem.* **81**, 33 (1999).
- [19] Y. Wang and P. Dea, *J. Chem. Eng. Data* **54**, 1447 (2009).
- [20] E. Wachtel, D. Bach, I. R. Miller, and N. Borochoy, *Chem. Phys. Lipids* **147**, 14 (2007).
- [21] L. Lobbecke and G. Cevc, *Biochim. Biophys. Acta* **1237**, 59 (1995).
- [22] J. Zeng, K. E. Smith and P. L. G. Chong, *Biophys. J.* **65**, 1404 (1993).
- [23] T. Yoshida, Y. Yamamoto, and K. Taga, *J. Phys. Chem. B* **107**, 3196 (2003).
- [24] A. N. Dickey and R. Faller, *Biophys. J.* **93**, 2366 (2007).
- [25] E. Terama, O. H. S. Ollila, E. Salonen, A. C. Rowat, C. Trandum, P. Westh, M. Patra, M. Karttunen, and I. Vattulainen, *J. Phys. Chem. B* **112**, 4131 (2008).
- [26] M. Orsi, W. E. Sanderson, and J. W. Essex, *J. Phys. Chem. B* **113**, 12019 (2009).
- [27] A. L. Frischknecht and L. J. D. Frink, *Biophys. J.* **91**, 4081 (2006).
- [28] J. M. Rodgers, M. Webb, and B. Smit, *J. Chem. Phys.* **132**, 064107 (2010).
- [29] D. T. Nizza and K. Gawrisch, *Gen. Physiol. Biophys.* **28**, 140 (2009).
- [30] H. V. Ly and M. L. Longo, *Biophys. J.* **87**, 1013 (2004).
- [31] Y. R. Shen, *The Principles of Nonlinear Optics*, New York: Wiley, (1984).
- [32] E. T. Castellana and P. S. Cremer, *Surf. Sci. Rep.* **61**, 429 (2006).
- [33] A. G. Lambert, P. B. Davies, and D. J. Neivandt, *Appl. Spectrosc. Rev.* **40**, 103 (2005).
- [34] S. Gopalakrishnan, D. F. Liu, H. C. Allen, M. Kuo, and M. J. Shultz, *Chem. Rev.* **106**, 1155 (2006).
- [35] H. F. Wang, W. Gan, R. Lu, Y. Rao, and B. H. Wu, *Int. Rev. Phys. Chem.* **24**, 191 (2005).
- [36] P. B. Miranda and Y. R. Shen, *J. Phys. Chem. B* **103**, 3292 (1999).
- [37] X. Zhuang, P. B. Miranda, D. Kim, and Y. R. Shen, *Phys. Rev. B* **59**, 12632 (1999).
- [38] D. H. Gracias, Z. Chen, Y. R. Shen, and G. A. Somorjai, *Acc. Chem. Res.* **32**, 930 (1999).
- [39] Z. Chen, Y. R. Shen, and G. A. Somorjai, *Annu. Rev. Phys. Chem.* **53**, 437 (2002).
- [40] F. G. Moore and G. L. Richmond, *Acc. Chem. Res.* **41**, 739 (2008).
- [41] G. L. Richmond, *Annu. Rev. Phys. Chem.* **52**, 357 (2001).
- [42] S. J. Ye, K. T. Nguyen, S. Le Clair, and Z. Chen, *J. Struct. Biol.* **168**, 61 (2009).
- [43] X. Chen, M. L. Clarke, J. Wang, and Z. Chen, *Int. J.*

- Mod. Phys. B **19**, 691 (2005).
- [44] X. Chen and Z. Chen, *Biochim. Biophys. Acta* **1758**, 1257 (2006).
- [45] A. Perry, C. Neipert, B. Space, and P. B. Moore, *Chem. Rev.* **106**, 1234 (2006).
- [46] C. T. Williams and D. A. Beattie, *Surf. Sci.* **500**, 545 (2002).
- [47] M. Buck and M. Himmelhaus, *J. Vac. Sci. Technol. A* **19**, 2717 (2001).
- [48] M. J. Shultz, C. Schnitzer, D. Simonelli, and S. Baldelli, *Int. Rev. Phys. Chem.* **19**, 123 (2000).
- [49] C. D. Bain, *J. Chem. Soc., Faraday Trans.* **91**, 1281 (1995).
- [50] S. J. Ye, K. T. Nguyen, and Z. Chen, *J. Phys. Chem. B* **114**, 3334 (2010).
- [51] S. J. Ye, H. C. Li, F. Wei, J. Jasensky, A. P. Boughton, P. Yang, and Z. Chen, *J. Am. Chem. Soc.* **134**, 6237 (2012).
- [52] H. C. Li, S. J. Ye, F. Wei, S. L. Ma, and Y. Luo, *Langmuir* **28**, 16979 (2012).
- [53] S. J. Ye and F. Wei, *Analyst* **136**, 2489 (2011).
- [54] S. J. Ye, G. M. Liu, H. C. Li, F. G. Chen, and X. W. Wang, *Langmuir* **28**, 1374 (2012).
- [55] W. R. Klem, *Alcohol* **15**, 249 (1998).
- [56] L. K. Tamm and U. A. Tatulian, *Quart. Rev. Biophys.* **30**, 365 (1997).
- [57] L. Yurttas, B. E. Dale, and W. R. Klem, *Alcohol. Clin. Exp. Res.* **16**, 863 (1992).
- [58] J. E. Bertie and S. L. Zhang, *J. Mol. Struct.: THEOCHEM* **413-414**, 333 (1997).
- [59] S. Dixit, W. C. K. Poon, and J. Crain, *J. Phys.: Condens. Matter* **12**, L323 (2000).
- [60] H. Chen, W. Gan, R. Lu, Y. Guo, and H. F. Wang, *J. Phys. Chem. B* **109**, 8064 (2005).
- [61] G. Ma and H. C. Allen, *J. Phys. Chem. B* **107**, 6343 (2003).
- [62] J. Sung, K. Park, and D. Kim, *J. Phys. Chem. B* **109**, 18507 (2005).
- [63] J. Sung and D. Kim, *J. Phys. Chem. C* **111**, 1783 (2007).
- [64] R. Superfine, J. Y. Huang, and Y. R. Shen, *Phys. Rev. Lett.* **66**, 1066 (1991).
- [65] X. K. Chen, W. Hua, Z. S. Huang, and H. C. Allen, *J. Am. Chem. Soc.* **132**, 11336 (2010).